Review

Joule heating and determination of temperature in capillary electrophoresis and capillary electrochromatography columns

Anurag S. Rathore*

Process Development, Amgen Inc., 30 W-2-A, One Amgen Center Drive, Thousand Oaks, CA 91320, USA

Abstract

This article reviews the progress that has taken place in the past decade on the topic of estimation of Joule heating and temperature inside an open or packed capillary in electro-driven separation techniques of capillary electrophoresis (CE) and capillary electrochromatography (CEC), respectively. Developments in theoretical modeling of the heat transfer in the capillary systems have focused on attempts to apply the existing models on newer techniques such as CEC and chip-based CE. However, the advent of novel analytical tools such as pulsed magnetic field gradient nuclear magnetic resonance (NMR), NMR thermometry, and Raman spectroscopy, have led to a revolution in the area of experimental estimation of Joule heating and temperature inside the capillary via the various noninvasive techniques. This review attempts to capture the major findings that have been reported in the past decade.
© 2004 Elsevier B.V. All rights reserved.

Keywords: Reviews; Joule heating; Electrochromatography; Capillary electrophoresis

Contents

1. Introduction

Joule heating in capillaries and columns used in electro-driven separation techniques such as capillary electrophoresis (CE) and capillary electrochromatography (CEC) are

know to affect the electroosmotic flow (EOF), retention/electrophoretic interactions, diffusion of analytes, and ultimately the efficiency and reproducibility of the separation [1,2]. Non-linear relationships between current and potential drop across an open or packed capillary are common in the literature of capillary electrophoresis and capillary electrochromatography and several attempts have been made to model this non-linear behavior [3–11]. More

---

* Tel.: +1-805-447-4491; fax: +1-805-499-5008.
  E-mail address: arathore@amgen.com (A.S. Rathore).

recently, experimental studies examining these models *via* a variety of direct and indirect measurements have been published [12–18]. Such approaches include use of techniques such as flow field dynamics studies in open and packed segments of capillaries by direct motion encoding of fluid molecules using pulsed magnetic field gradient nuclear magnetic resonance (NMR) [16], NMR thermometry [17] and Raman spectroscopic measurements [18] for measuring temperature inside the open capillary or packed column.

This article reviews the progress that has taken place in the past decade on the topic of estimation of Joule heating and temperature inside an open or packed capillary in electro-driven separation techniques of CE and CEC, respectively. The scope of the review includes both the theoretical modeling of the heat transfer in the capillary systems, as well as, experimental studies that provide direct or indirect measurements of Joule heating and the temperature inside the capillary.

2. Theoretical studies

2.1. Flow of ions through open and packed capillaries

When an open tube with fixed charges at the tube wall is filled with an electrolyte solution, an electrical double layer is formed [19–22]. The double layer contains a higher concentration of counterions than the bulk solution and so to maintain electroneutrality, the bulk electrolyte outside has the same amount of excess coions. If ionic conduction through the bulk electrolyte is the dominant mechanism of ionic migration, the conductivity of an electrolyte filled cylindrical capillary, σ, is expressed as [23]:

$$\sigma = \frac{iL}{VA} \tag{1}$$

where i is the current flowing through a capillary of length, L, and cross-sectional area, A, when a potential drop, V, is applied across the capillary. The conductivity of an electrolyte solution is independent of the dimensions of the capillary tube and can be expressed in terms of the concentration charge and mobility of the constituent ions as follows [21,23]:

$$\sigma_{open} = F^2 C \sum_j z_j^2 \nu_j x_j \tag{2}$$

where F is the Faraday constant, C is the molar concentration of the buffer and z_j, ν_j and x_j are the valency, mobility and number of moles of jth ionic species per mole of buffer. It follows from Eq. (2) that the conductivity of sufficiently dilute electrolytes increases linearly with the molar concentration of the electrolyte.

In absence of Joule heating and other non-linear effects, the conductivity of an ionic solution is a constant and so

current varies linearly with the applied potential drop and the electric field strength according to the following expression:

$$i = \left(\frac{\sigma A}{L} \right) V = (\sigma A)E \tag{3}$$

where E is the electric field strength across the capillary.

For the case of CEC, in order to simplify the analysis of a column that is completely packed, it can be represented by a hypothetical open tube [23]. This tube has the same length, L, as that of the packed column, but has an equivalent conductivity, σ_e, that accounts for the geometrical characteristics of the packed column. This case can be represented as follows:

$$i = \left(\frac{\sigma_e A \varepsilon}{L} \right) V \tag{4}$$

where ε is the column porosity and accounts for the reduced free cross-sectional area in a packed column, and conductivity (σ_e) of this hypothetical tube is an empirical quantity that needs to be calculated from current–voltage measurements with the packed column.

2.2. Effect of Joule heating on flow of ions

Power dissipation in the capillary has been known to cause heating of the electrolyte, a phenomenon often referred to as Joule heating [3–11]. The amount of heat generated in an electrical system can be simply calculated using the following expression:

$$J(t) = iVt = i^2 Rt = \frac{V^2 t}{R} = \frac{V^2 \sigma A t}{L} \tag{5}$$

where J is the heat generated (Joules) as a function of time (seconds), t, when a potential drop is applied across a capillary of resistance, R, area of cross-section, A, and length, L. This heat is dissipated across the capillary wall *via* natural or forced cooling. It follows from Eq. (5) that the problem of Joule heating gets worse with increasing capillary diameter, potential drop, and time.

In the presence of the electroosmotic flow in an open capillary, ions can be transported through convective as well as conductive mechanisms. The convective mechanism can be ignored if [6]:

$$\frac{du_{eo}\rho c_p}{\lambda} < 3 \tag{6}$$

where d is the capillary diameter, u_{eo} the electroosmotic flow velocity, and ρ, c_p, and λ are (respectively) the density, specific heat capacity, and thermal conductivity of the buffer solution. For most CE and CEC systems, the left hand side in Eq. (6) is of the order of 10^{-3} and so the condition in Eq. (6) is always satisfied. For such systems, the temperature profile in the capillary can be assumed to be axially uniform through the capillary. However, as Morris and co-workers have reported [18], if there is a temperature sink (such as a metal plate) in touch with the capillary end, the resulting end effects could be appreciable.

The above-mentioned conclusions are also applicable to packed capillaries in CEC if the packing is non-conductive and surface conductivity through the double layer around the particles is negligible [23].

2.3. Calculation of temperature increase in capillary electrophoresis

Several attempts have been made to model the effects of Joule heating and to calculate the resulting temperature profile in a CE capillary [3–11]. In this section, we will review these models and summarize the key findings that have taken place in this area.

Cohen et al. [2] suggested that if radial diffusion is slow, Joule heating will cause the solute molecules near the center of the capillary to migrate faster than those near the wall leading to band broadening. If the heat is not well dissipated, the temperature difference between the center and wall of the capillary at high voltages can be >50 °C leading in some cases to drying of the capillary. The authors concluded that reproducible CE separations would require temperature control and possibly, a careful selection of buffers.

Grushka et al. [6] examined the effect of temperature gradients on efficiency of CE separations in 1989. They proposed that for a fused silica capillary with a polyimide coating, the wall temperature is given by:

$$T_{\rm w} = T_{\rm o} + \frac{JR_{\rm i}^2}{2}\left[\frac{1}{\chi_{\rm s}}\ln\left(\frac{R}{R_{\rm i}}\right) + \frac{1}{\chi_{\rm c}}\ln\left(\frac{R_{\rm o}}{R}\right) + \frac{1}{R_{\rm o}h}\right] \quad (7)$$

where $T_{\rm w}$ is the temperature at the capillary wall, $T_{\rm o}$ the ambient temperature, and $\chi_{\rm s}$ and $\chi_{\rm c}$ are the thermal conductivities of the fused silica and polyimide coating, respectively. Also, h is the heat transfer coefficient to the surroundings, $R_{\rm i}$, R and $R_{\rm o}$ are capillary radii corresponding to the inside of the capillary, without polyimide coating and with polyimide coating, respectively. Based on the theoretical treatment, it was proposed that Joule heating would lead to a temperature dependence of the velocity, which in turn would cause a loss in efficiency of separation at higher temperatures. This loss would be particularly significant for large solutes due to their small diffusion coefficients and at high voltages when the flow velocity is high.

In 1990, Gobie and Ivory [9] published a thermal model of CE that took into account the "autothermal effect" and their calculations yielded a higher temperature inside the capillary than predicted by the constant conductivity model used in the above-mentioned treatment by Grushka et al. They used the linear model of electrical conductivity (σ) due to its simplicity and ability to offer a good approximation between 10–20 °C such that:

$$\sigma = \sigma_{\rm o}[1 + \alpha(T - T_{\rm o})] \quad (8)$$

where T is the temperature of the buffer in the capillary, α the temperature coefficient of conductivity and $\sigma_{\rm o}$ the conductivity measured at the reference temperature, $T_{\rm o}$.

The Gobie Ivory model for natural convection air-cooled capillaries, when the autothermal parameter (k) is small, can be summarized as follows [9]:

$$\theta = \frac{(1/4)(1-\eta^2) + (k^2/64)(\eta^4-1) + (1/Bi_{\rm oA})(1 - k^2/8)}{f(k)} \quad (9)$$

with

$$\theta = \frac{T - T_{\rm o}}{\Delta T_{\rm ref}} \quad (10)$$

$$\eta = \frac{r}{R_{\rm i}} \quad (11)$$

$$Bi_{\rm oA} = \frac{hR_{\rm i}}{\chi} \quad (12)$$

$$\Delta T_{\rm ref} = \frac{\sigma_{\rm o}AV^2}{\pi\chi L^2} \quad (13)$$

$$k = \sqrt{\alpha\,\Delta T_{\rm ref}} \quad (14)$$

where θ is dimensionless temperature, η dimensionless radial coordinate, k the autothermal parameter, $\Delta T_{\rm ref}$ the characteristic temperature difference, $Bi_{\rm oA}$ the Biot number, L the length of the capillary, A the free cross-sectional area of the capillary, and χ the thermal conductivity of the buffer solution. The Biot number is often used to characterize the heat transfer across the capillary from the internal heated buffer to the surrounding capillary wall and external coolant. The Biot number reaches a maximum when heat is produced within the capillary at an equal or higher rate than it can be dissipated.

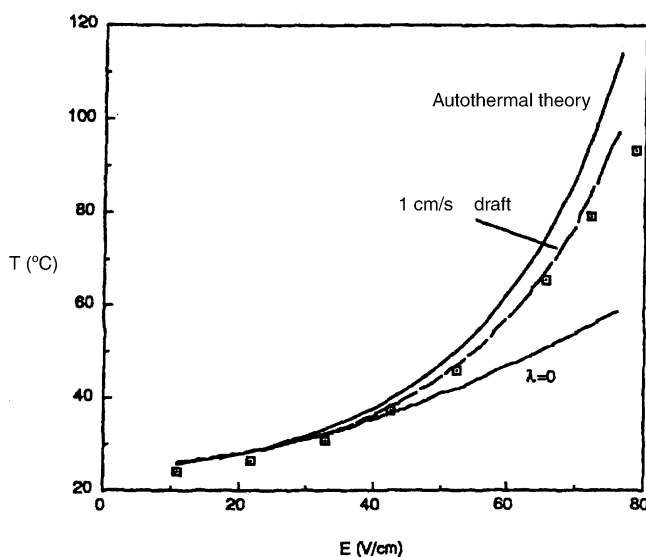Fig. 1 shows a comparison between experimental data and the predictions from the autothermal theory as stated

Fig. 1. Comparison of experimentally measured capillary temperature and theory for the 250 μm × 350 μm capillary. This figure also shows the effect of a 1 cm s^{-1} draft on the predicted capillary temperature. Adapted from [9].

in Eq. (9) and the constant-conductivity model as given by Eq. (7). It is seen that the autothermal theory overestimates the capillary temperature, while the constant-conductivity model underestimates it. The discrepancy between the experimental data and the predictions of the autothermal theory were assigned to the slow circulation of air inside the apparatus. It was seen that if air circulation was increased, the difference became smaller. It is clear from Fig. 1 that temperature increases of up to 80 °C can take place in a CE system, depending on the selection of buffer, experimental conditions such as voltage and capillary length, and the effectiveness of cooling mechanism used in the apparatus.

Bello and Righetti gave a thorough examination to the issue of heat transfer in CE through a series of papers published in 1992 [3,4,10,11]. They pointed out that the Gobie–Ivory theory required precise knowledge of diameters of the capillary lumen, fused-silica wall and polyimide coating, measurement of all of which would require considerable efforts. Instead, they suggested a procedure of electrochemical calibration of a capillary based on their approximate thermal theory [10,11]. After measurements of current at low and high voltages, this procedure facilitates calculation of the current–voltage and temperature–voltage dependences, and also of the capillary inner diameter if the specific conductivity of the buffer solution is known.

The Bello–Righetti model can be summarized by the following equation for the average buffer temperature inside the capillary [3]:

$$T = T_o + \frac{\Delta T_{ref}}{2Bi'_{oA} - k^2} \tag{15}$$

where the Biot number used, Bi'_{oA}, is the average of experimentally determined Biot numbers at 25 and 30 kV and can be expressed as:

$$Bi_{oA} = \frac{k^2}{2(1 - \sigma_o/\sigma)} \tag{16}$$

Fig. 2 shows a plot comparing the results from the Bello–Righetti model for two buffer systems: the phosphate and the acetate buffers. It is seen that the buffer electrical conductivity has a very significant effect on the average temperature. They recommended that, due to their smaller electrical conductivities, the zwitterionic buffers should be used in CE.

In 1994, Knox and McCormack [8] investigated the temperature effects in CE using capillary cooled by natural convection and confirmed that the self heating of the capillary is primarily responsible for these effects. They examined the extent of self-heating by a variety of methods and concluded that to the first approximation it is proportional to the power dissipation in the capillary. They proposed that upon increasing temperature, the resulting decrease in viscosity is responsible for the non-linearity in velocity–field strength relationship, while the increase in diffusion coefficient is responsible for poor separation efficiencies at elevated tem-
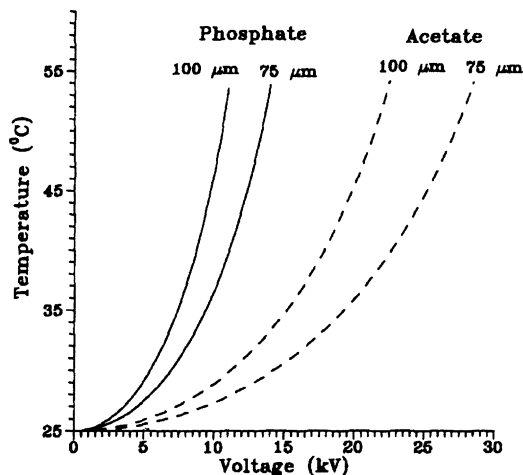

Fig. 2. Temperature voltage plots for phosphate (—) and acetate (- - -) buffers. Adapted from [3].

peratures. They proposed the following expression for the temperature of the buffer inside the capillary [8]:

$$T = T_o + 1.273 \frac{Ei}{d^{0.3}} \tag{17}$$

While the qualitative conclusions of all the investigations mentioned in this section are very similar, the actual expressions for measurement of the temperature inside the capillary are significantly different, partly due to the different sets of assumptions that were undertaken. While applying these equations, the researcher should thoroughly check to make sure that these assumptions are applicable to his/her apparatus. In the following section, we will review the various experimental studies that have reported agreement or discrepancies in the above-mentioned treatments.

2.4. Calculation of temperature increase in capillary electrochromatography

Rathore et al. [1] recently applied the Bello–Righetti model for the case of packed columns that are used in CEC. The model was chosen because of its accurate representation of the different processes that occur in the separation system, as well as, its mathematical simplicity in calculation of the temperature from measurements of current and conductivity at different voltages. It was assumed that the packed segment can be replaced by a hypothetical open tube [23] and so the above-mentioned expressions can be rewritten as follows [1]:

$$\sigma_e = \sigma_{e,o}[1 + \alpha(T - T_o)] \tag{18}$$

$$Bi_{oA} = \frac{k^2}{2(1 - \sigma_{e,o}/\sigma_e)} \tag{19}$$

$$\Delta T_{ref} = \frac{\sigma_{e,o}AV^2\varepsilon}{\pi\chi L^2} \tag{20}$$

$$T = T_o + \frac{\Delta T_{ref}}{2Bi'_{oA} - k^2} \qquad (21)$$

Eq. (21) can be used to calculate the temperature inside a capillary column in CEC.

2.5. Conductivity–electric field strength relationships in capillary electrophoresis and capillary electrochromatography

As discussed in the above sections, Joule heating caused by the power dissipation leads to an increase in the temperature of the electrolyte inside the capillary and, thus, higher ionic mobilities. This results in increasing electrical conductivity of the buffer at higher potential drops. It follows then from Eq. (3) that the relationship between the current and the potential drop becomes a non-linear relationship with the current increasing disproportionately at higher voltages in comparison to that predicted by a linear relationship. These effects of the Joule heating on the conductivity have been modeled and the following relationship has been proposed by Yu and Davis [5]:

$$\sigma = \sigma_o + a'E^3 \qquad (22)$$

where, a' is a constant and, as defined earlier, σ_o the conductivity as measured at very low voltages at the reference temperature, $T_o = 25\,^{\circ}C$. It follows then from Eqs. (3) and (22) that the plot of current as a function of voltage would result in a non-linear relationship, with the non-linearity increasing with increase in potential drop.

3. Experimental studies

3.1. Joule heating in capillary electrophoresis

Llu et al. [18] published Raman spectroscopic measurement of spatial and temporal temperature gradients in CE capillaries in 1994. They showed that Raman spectroscopy could be effectively used as a noninvasive method that could perform time-resolved, diffraction limited spectral imaging along or across the capillary with a time resolution of 1–2 s. Fig. 3 shows a comparison of the increase in capillary temperature upon application of voltage as measured by (A) the Raman spectroscopic method and (B) by change in conductance of the buffer. It is seen that the Raman method provides a quicker measure of temperature increase with the conductance method showing steady state in capillary temperature almost 10 s later.

Cross and Cao [12] used five sulphonamides as probes to study the effect of increasing buffer concentration on electrophoretic mobility in CE. They measured the effect of elevated temperature on degree of ionization and viscosity and used the electrophoretic mobility measurements to estimate mean internal capillary temperatures. Their results are presented in Fig. 4 and it is seen that with decreasing buffer
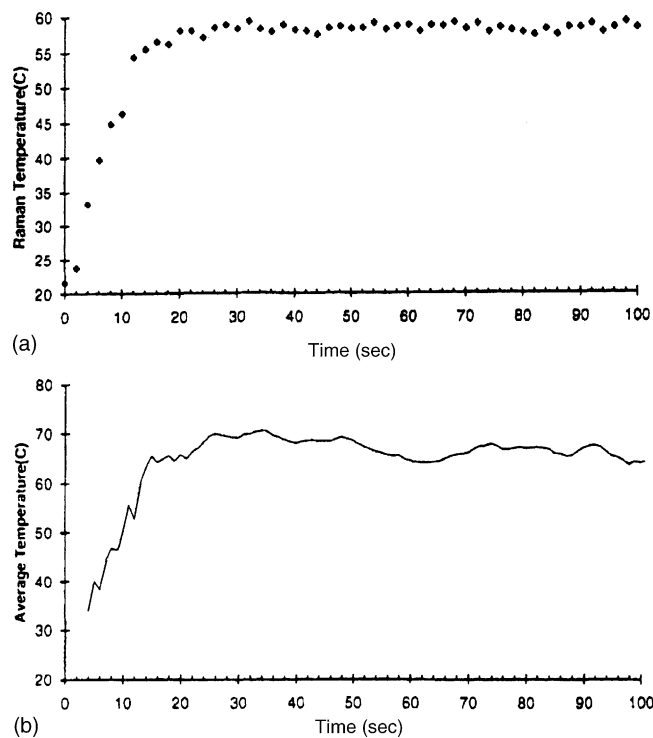

Fig. 3. Initial capillary temperature transient. Capillary dimensions: 37.5 μm lumen, 142.5 μm wall, and 12 μm polymer coating. Capillary length is 1 m and heat sinks are at 0 and 25.4 cm. Buffer is 0.025 M phosphate, pH 7.4. Field strength 310 V cm^{-1}. (A) Raman temperature rise as a function of time. (B) Conductance change as a function of time. Time zero is the imposition of the driving voltage. Adapted from [18].

concentrations, the electrical resistance increases leading to lower power dissipation and less internal heating. However, the increases in temperature predicted in this study were found to be approximately one fourth of what was predicted by the above-mentioned treatment of Knox and McCormack [8]. The authors suggested that this discrepancy was perhaps due to the differences in the two apparatus. While their system used forced cooling system such that heat dissipation was very efficient, the Knox–McCormack apparatus used natural convection for cooling.

In 2000, Lacey et al. [17] used nanoliter-volume proton nuclear magnetic resonance spectroscopy to monitor the electrolyte temperature in CE. By measuring the shift in the proton resonance frequency of the water signal, they were able to record the temperature inside the capillary in a noninvasive fashion with subsecond temporal resolution and spatial resolution of the order of 1 mm. They observed temperature increases of more than 65 °C under typical CE conditions. Table 1 presents measurement of the intracapillary temperature by the Gobie–Ivory method [9], Raman spectroscopy [18] and NMR [17]. It is seen that the three methods are in very close agreement with each other and show substantial amount of Joule heating under the chosen experimental conditions. This is further illustrated in Fig. 5, where it is seen that an increase in power generation leads to longer times required to reach steady state. This is due to
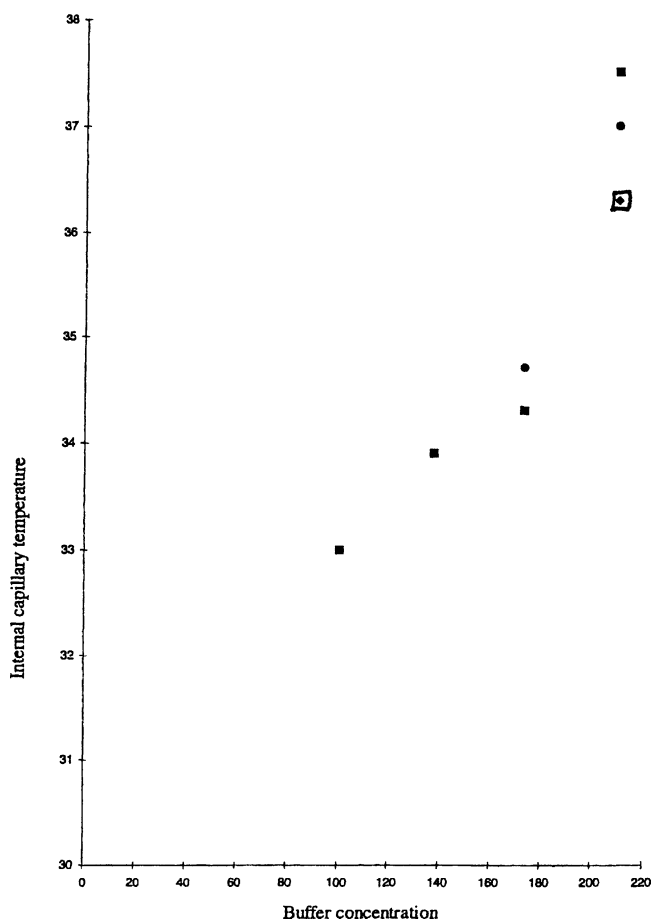
Fig. 4. Mean internal capillary temperatures estimated from electrophoretic mobility deviations from dilute solution behaviour for sulphonamide analytes plotted as a function of the buffer concentration (mM). Legend: (□) sulphamethazine, (■) sulphamethizole, and (●) phthalyl sulphacetamide. Adapted from [12].

the inability of the system to dissipate heat at the rate it is being generated.

Tallarek et al. [16] investigated the flow field dynamics in open and packed segments of capillary columns by a direct motion encoding of the fluid molecules using pulsed magnetic field gradient NMR. They found temperature increase of ∼16 °C above ambient at the highest power level

Table 1
Intracapillary temperatures as determined by theory, Raman and NMR

Power/length (W m^{-1})	Gobie and Ivory (°C)	Raman (°C)	NMR (°C)
0.161	27.1	27.1	25.9
0.408	30.2	30.8	29.4
0.813	35.5	36.2	35.0
1.504	44.2	44.6	44.6
2.765	60.1	60.8	62.1

The values for the calculated temperatures from the theory of Gobie and Ivory are obtained for 75 μm i.d. × 375 μm o.d. PTFE-coated capillaries. NMR temperatures were determined at these power levels by using the regression fit for the 50 μm i.d. × 360 μm o.d. capillary with 50 mM phosphate buffer in water. Adapted from [17].
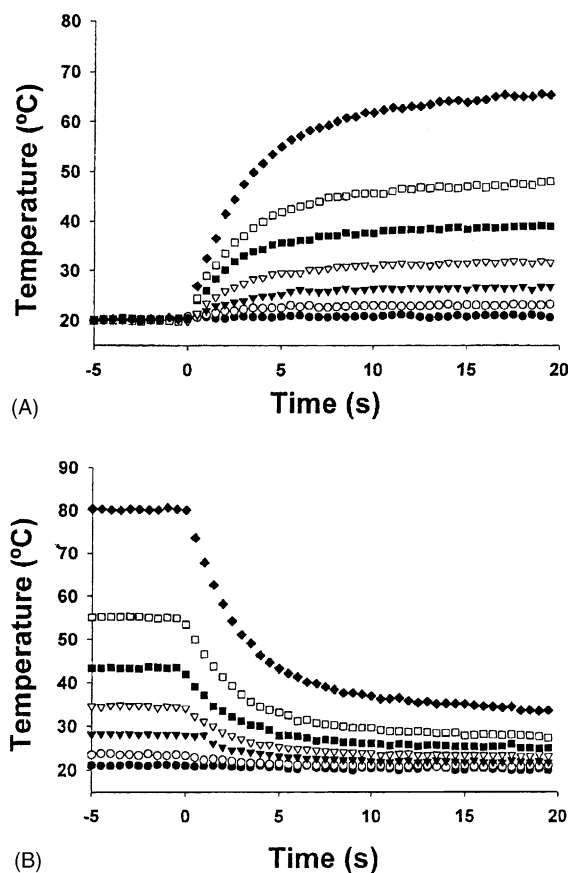

Fig. 5. Temperature as a function of time for a 38 cm long, 50 μm i.d., 360 μm o.d. fused-silica capillary filled with 50 mM phosphate buffer in water. (A) Time zero corresponds to the point at which a voltage is applied and maintained across the capillary. The symbols denote the applied voltage: (●) −2 kV; (○) −4 kV; (▼) −6 kV; (□) −8 kV; (■) −10 kV; (□) −12 kV; and (□) −15 kV. (B) Time zero corresponds to discontinuation of a voltage which had been applied for the previous 5 min. The symbols denote the magnitude of the applied voltage: (●) −2 kV; (○) −4 kV; (▼) −6 kV; (□) −8 kV; (■) −10 kV; (□) −12 kV; and (□) −15 kV. Adapted from [17].

in the capillary ($Ei = 2.42$ W m^{-1} at $E = 31.4$ kV m^{-1} and $i = 77$ μA). Also, they concluded that if the temperature increase is <25 °C, radial gradients are small and the associated Taylor dispersion can be ignored.

Palonen et al. [13] published a study in 2001 to investigate the effect of high electric field on the separation of basic analytes in non-aqueous alcohol background electrolyte (BGE) solution. They also used the Knox–McCormack model [8] for estimating the temperature inside the capillary and these calculated temperatures are presented in Table 2. They found that the deteriorating self-heating effect was strongest with the methanol BGE solution and smaller for propanol and butanol BGEs, emphasizing on the importance of choosing the solvent for the BGE when planning CE experiments.

Swinney and Bornhop [14] presented the use of picoliter volume interferometer to measure the extent of Joule heating in chip-scale CE. The configuration of their detector consisted of an unfocused laser, an unaltered silica

Table 2
Estimates of the temperature in the capillary at different separation voltages[a]

U (kV)	T_s and T_c (°C)[b]			
	MeOH	EtOH	PrOH	BuOH
20	25.0 (25.6)	23.4 (23.6)	– (–)	– (–)
25	26.3 (27.2)	23.7 (23.9)	23.1 (23.2)	23.0 (23.0)
30	27.9 (29.3)	24.0 (24.4)	23.2 (23.3)	23.0 (23.1)
35	30.0 (32.0)	24.4 (24.9)	23.3 (23.4)	23.1 (23.1)
40	32.6 (35.4)	24.9 (25.6)	23.4 (23.5)	23.1 (23.1)
45	35.8 (39.5)	25.5 (26.3)	23.5 (23.7)	23.1 (23.2)
50	39.5 (44.3)	26.0 (27.0)	23.7 (23.9)	23.2 (23.2)
55	– (–)	– (–)	23.8 (24.1)	23.2 (23.3)
60	50.1 (58.0)	27.7 (29.2)	24.0 (24.3)	23.3 (23.4)

Adapted from [13].

[a] Temperatures at the capillary surface (T_s) and centre (T_c) were calculated.

[b] Flow velocity of the air coolant, $3.8\,\mathrm{m\,s^{-1}}$; capillary outer diameter, $375\,\mu\mathrm{m}$; external capillary radius, $172.5\,\mu\mathrm{m}$; kinematic viscosity, $0.153\,\mathrm{cm^2\,s^{-1}}$; Reynold's number, 93; thermal conductivities of cooling medium, $0.02604\,\mathrm{W\,m^{-1}\,K^{-1}}$; MeOH BGE, $0.2028\,\mathrm{W\,m^{-1}\,K^{-1}}$; EtOH BGE, $0.1742\,\mathrm{W\,m^{-1}\,K^{-1}}$; PrOH BGE, $0.1557\,\mathrm{W\,m^{-1}\,K^{-1}}$; BuOH BGE, $0.1535\,\mathrm{W\,m^{-1}\,K^{-1}}$; quartz wall, $1.38\,\mathrm{W\,m^{-1}\,K^{-1}}$; polyimide coating, $0.1550\,\mathrm{W\,m^{-1}\,K^{-1}}$.

chip with a half-cylinder channel and a photodetector. Using such a setup, they were able to detect temperature changes associated with Joule heating in on-chip CE system for 90 and 40 μm deep channels. They observed a 7% reduction in separation efficiency with Tris–boric acid buffer at electric field strengths of $400\,\mathrm{V\,cm^{-1}}$. A comparison of their experimental results with the predictions from Knox–McCormack expression is presented in Table 3. While the Knox–McCormack method yielded accurate estimations at low electric fields, it overestimated the temperature at higher electric field strengths. The authors proposed that the discrepancy is due to the differences between the buffer systems used in the two studies.

Recently, Rathore et al. [1] investigated Joule heating in CE and CEC [1]. Fig. 6 illustrates Ohm's plots for open tubes having inner diameters of 75, 50, and 12 μm using two different mobile phases, acetonitrile–100 mM Tris, pH 8 (80:20, v/v) and acetonitrile–50 mM Tris, pH 8 (80:20, v/v). The positive deviation from linearity is obvious in the
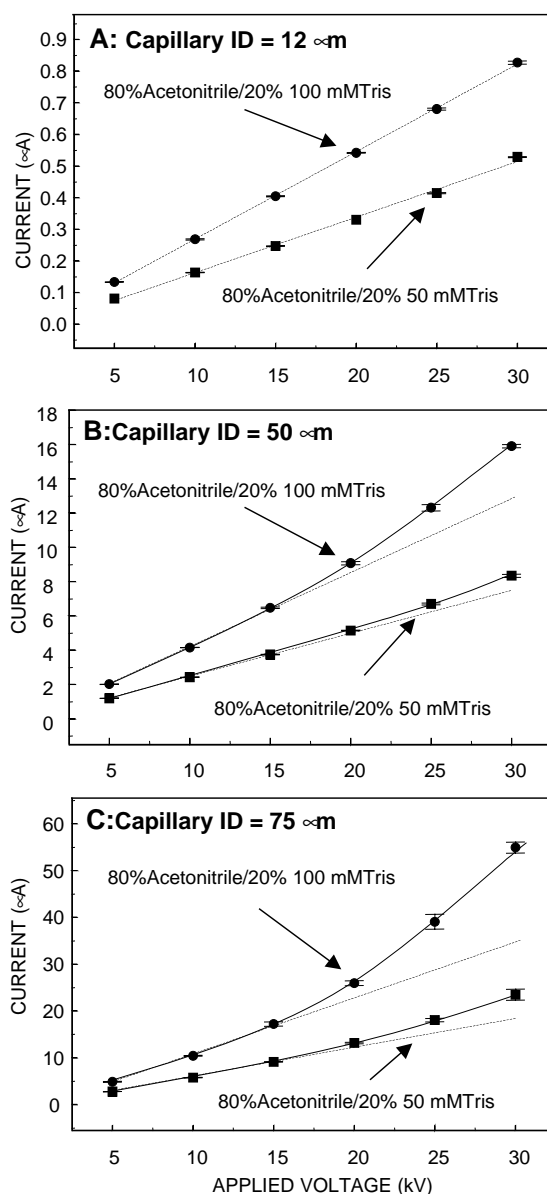

Fig. 6. Ohm's plots for: (A) 12 μm, (B) 50 μm, and (C) 75 μm i.d. capillaries. The Tris buffers solution had a pH = 8. Capillary length in all cases was 30 cm. Adapted from [1].

Table 3
Comparison of experimentally measured and theoretically predicted operating temperatures

	Buffer			
	100 mM Tris–30 mM boric acid		20 mM HEPES	
Conductivity (μS cm^{-1})		525.3		36.4
Electric field strength (V cm^{-1})	240	475	240	475
Current (μA)	5.3	10.6	0.37	0.73
Change in viscosity (cP)	0.035	0.065	0.004	0.01
% change in viscosity	3.5%	6.5%	0.4%	1.7%
Experimental ΔT (°C)	1.48	2.81	0.16	0.69
Theoretical ΔT (°C)	1.43	5.66	0.10	0.39
Thermal equilibrium time (s)	2.7 ± 0.2	2.6 ± 0.1	0.9 ± 0.1	1.1 ± 0.1

Adapted from [14]. HEPES: 4-(2-hydroxyethyl)-1-piperazinethanesulfonic acid.

A : Buffer –80% AcN/20% 50 mMTris
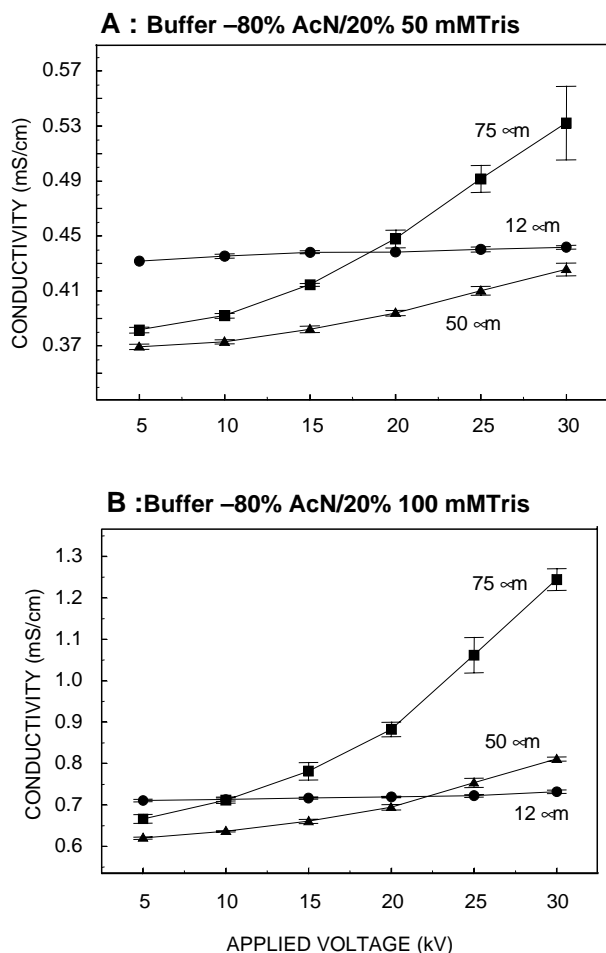

B :Buffer –80% AcN/20% 100 mMTris

Fig. 7. Conductivity plots for 12, 50, and 75 μm i.d. capillaries. The mobile phases used were: (A) acetonitrile–50 mM Tris (80:20) and (B) acetonitrile–20% 100 mM Tris (80:20). Other conditions as in Fig. 6. Adapted from [1].

case of the 75 μm i.d. capillary, and perhaps less so for the 50 μm i.d. capillary and is indicative of inadequate dissipation of Joule heating in these two systems. This is further elucidated by Fig. 7 that shows changes in conductivity as a
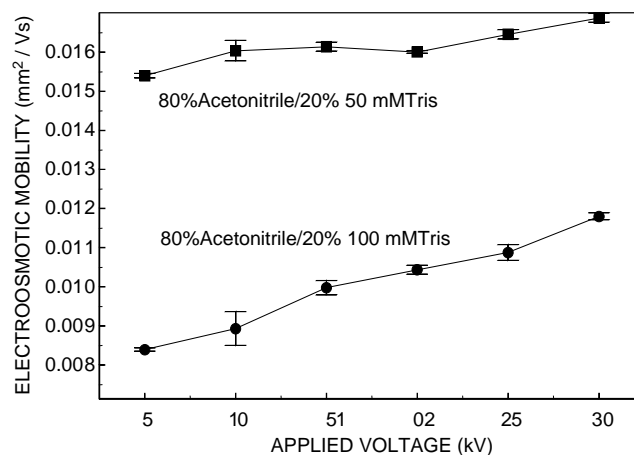

Fig. 8. Electrosmotic mobility observed in 50 μm open tubes. Conditions as in Fig. 6. Adapted from [1].

function of voltage. In absence of Joule heating, conductivity plots should have a slope close to zero. Thus, an increase in conductivity with applied voltage as seen in Fig. 7 is indicative of presence of Joule heating in the system. The flat slope of the conductivity plot for the 12 μm i.d. column indicates excellent heat dissipation in this tube, in agreement with the Ohm's plot. Therefore, the authors suggested the use of conductivity plots instead of Ohm's plots to assess column heating.

Rathore et al. [1] also measured and plotted electroosmotic mobility as a function of the applied voltage. This is presented in Fig. 8 and it is seen that using the 50 μm i.d. capillary and mobile phases containing 20% of 50 mM Tris and 20% of 100 mM Tris, respective increases of 10% and 40% in the mobilities are observed. They emphasized that the mobility dependence on applied field needs to be recognized for obtaining reproducible separations. Further, they measured electrical conductivity for different buffers at different temperatures using a conductivity meter and, as shown in Table 4, calculated the temperature coefficient of conductivity, α, using Eq. (8). Using

Table 4
Calculation of the temperature coefficient of electrical conductivity, α, for different buffers used in the experiments using the conductivity meter; buffer pH = 8.0

Buffer	Temperature (°C)	Conductivity (mS cm^{-1})	Temperature coefficient of σ (K^{-1}) $\alpha = ((\sigma/\sigma_o) - 1)/(T - T_o)$	Average α (K^{-1})
MeCN–100 mM Tris (80:20) (total Tris 20 mM)	10	0.500		
	20	0.650	0.030	0.025
	30	0.780	0.020	
MeCN–50 mM Tris (80:20) (total Tris 10 mM)	10	0.290		
	20	0.370	0.028	0.024
	30	0.440	0.019	
MeCN–10 mM Tris (80:20) (total Tris 2 mM)	10	0.062		
	20	0.077	0.024	0.022
	30	0.093	0.021	

Adapted from [1].

Table 5
Calculation of theoretical temperature inside an open capillary at different voltages

Buffer	V (kV)	i (µA)	σ (mS cm^{-1})	ΔT_{ref} (K)	k	Bi'_{oA}	T (°C)
MeCN–100 mM Tris (80:20) (total Tris 20 mM)	5	4.96	0.674				25.0
	10	10.59	0.719	0.173	0.064		27.2
	15	17.47	0.791	0.389	0.097		30.3
	20	25.97	0.882	0.691	0.129		35.5
	25	37.85	1.029	1.080	0.161		44.2
	30	54.55	1.235	1.555	0.193	0.041	59.7
MeCN–50 mM Tris (80:20) (total Tris 10 mM)	5	2.81	0.382				25.0
	10	5.77	0.392	0.098	0.048		26.4
	15	9.15	0.414	0.220	0.073		28.2
	20	13.18	0.448	0.391	0.097		31.0
	25	18.09	0.492	0.611	0.121		35.2
	30	23.49	0.532	0.880	0.145	0.037	41.4
MeCN–10 mM Tris (80:20) (total Tris 2 mM)	5	0.50	0.068				25.0
	10	1.02	0.069	0.017	0.020		25.3
	15	1.54	0.070	0.039	0.031		25.8
	20	2.08	0.071	0.070	0.041		26.4
	25	2.62	0.071	0.109	0.051		27.2
	30	3.23	0.073	0.157	0.061	0.026	28.3

Capillary, 30 cm × 75 µm; buffer pH, 8.0; detection at 214 nm at 15 cm; thermal conductivity of solution, 0.61 W m^{-1} K^{-1} and temperature coefficient of electrical conductivity, α, as calculated in Table 4. Adapted from [1].

the Bello–Righetti model (Eqs. (13), (15) and (16)), they calculated the temperature inside the capillary and the results are presented in Table 5. Temperature increases of up to 35 °C were estimated, which are very close to what has been reported in other experimental studies mentioned above.

More recently, Porras et al. [15] investigated the influence of solvent on temperature and thermal peak broadening in CE. They estimated the temperatures inside the capillary from measured conductivities and compared them to the calculated temperature values using the above-mentioned models from Grushka et al. and from Bello and Righetti. As seen in Fig. 9, they found that the predictions from the two models were fairly consistent with each other and were in good agreement with the experimental findings when natural convection in still air is the sole cooling mechanism. For this case, temperature increases significantly even at relatively low voltages, with the aqueous solution showing the highest temperature increase as compared to organic solvents except with the 180 µm capillary where no difference was found between the solvents. For the cases where forced circulating air or liquid was used for cooling the capillary, the temperature increase is smaller than the case of still air. However, the temperatures calculated from measured conductivities are found to be significantly higher than the calculated temperature values from the theoretical models. The authors assigned this discrepancy to the fact that in most available CE apparatus almost 50% of the capillary is outside the thermostated cartridge and is exposed to still air. Hence, despite the expectation that the air/liquid cooled systems will have effective cooling, in reality the overall temperature in the capillary is still significantly higher than what is theoretically predicted and is often underestimated in practice.

Porras et al. also examined the temperature gradients in the different solvents and found that the temperature difference between center of the capillary and the inner wall is <1 °C in narrow tube even at the highest applied voltage, but can reach several degrees in a wide-bore capillary. This is minimal to the overall increase in capillary temperature and is in agreement with the conclusions of Tallarek et al. discussed above.

3.2. Joule heating in capillary electrochromatography

Rathore et al. [1] applied the above-mentioned theories and approaches that were developed for CE on estimation of Joule heating and temperature inside a capillary column for CEC. As seen in Fig. 10, data from packed columns using the same mobile phases show deviation from linearity in the same manner as seen for the open capillary in Fig. 6. The mobile phases used here have total Tris concentrations of 20 mM or 10 mM, and CEC is frequently run with mobile phases having ion concentrations in this range. The data indicates that the heat generated in these typical CEC mobile phases is not effectively dissipated in open tube systems or in an entirely packed column format. Using Eqs. (1) and (4) and experimental values of the current, the authors measured conductivity at different applied voltages and this relationship for a packed column is illustrated in Fig. 12. As discussed above, an increase in the measured conductivity upon increasing applied voltage signals ineffective dissipation of Joule heating and this is seen in the CEC column.
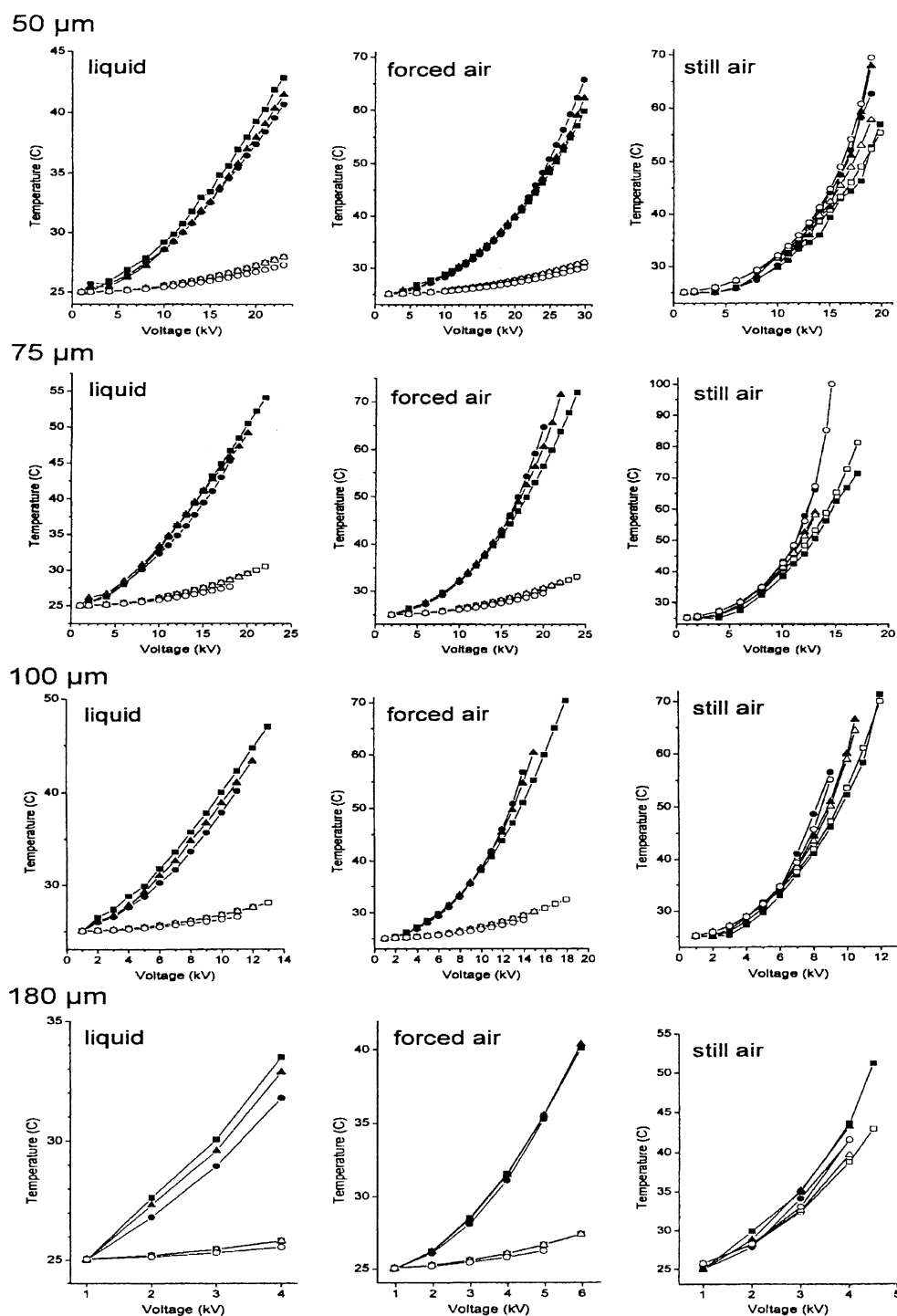
Fig. 9. Temperature of the electrolyte solution in the capillary averaged over the capillary length (full symbols), derived from measured conductivities, and mean temperature, T_{mean}, averaged over the capillary cross section (empty symbols). T_{mean} was calculated from the heat balance equation by iteration. Initial conductivity of the BGE: $0.517\,S\,m^{-1}$ at $25.0\,°C$. o.d. $375\,\mu m$, except for $180\,\mu m$ i.d. capillary. Solvents: ($\square$, $\blacksquare$) MeCN; ($\triangle$, $\blacktriangle$) MeOH; and ($\bigcirc$, $\bullet$) Water. Adapted from [15].

Rathore et al. also used the Bello–Righetti model to calculate the temperature inside the CEC column and these results are presented in Table 6. As expected from Eqs. (3), (8), and (18), the current and the conductivity increase with the potential drop and so does the predicted temperature inside the capillary. In almost all cases, the predicted temperature is higher at higher salt concentrations as Joule heating increases with salt concentration. The highest calculated
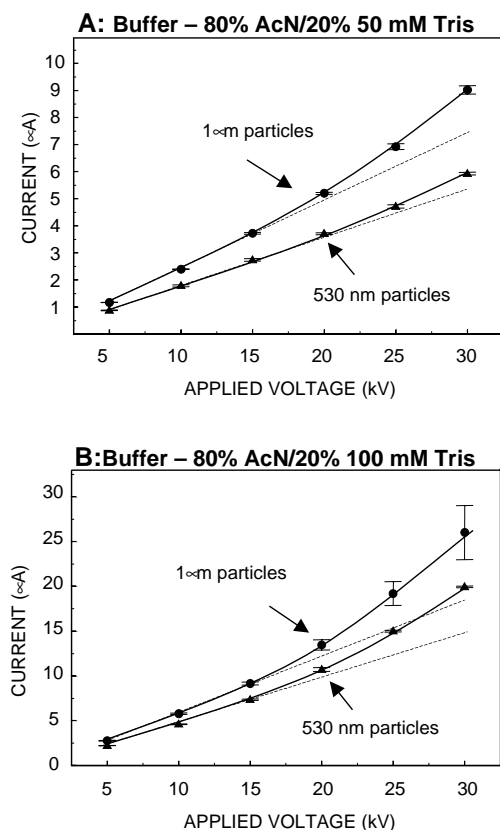
Fig. 10. Ohm's plots for 75 μm i.d. packed capillaries, capillary length in both cases was 15 cm, entirely packed, with particle size as indicated. (A) Acetonitrile–50 mM Tris (80:20) and (B) acetonitrile–100 mM Tris at pH = 8 (80:20). The Tris buffers solution had a pH = 8. Adapted from [1].

temperature for their experiments was about 47 °C, seen in the case when a potential drop of 30 kV is applied across a 15 cm long and 75 μm diameter capillary packed with 1 μm silica particles and filled with a mobile phase of MeCN–100 mM Tris (80:20). This is very consistent with temperature rises that have been reported in recently published experimental findings using pulsed magnetic field gradient nuclear magnetic resonance, NMR thermometry, and Raman spectroscopic measurements [16–18]. It follows that for higher ionic concentrations or capillary diameters, Joule heating could become a real issue in CEC and for such cases attention must be paid to designing an efficient heat removal mechanism in order to have a robust CEC system.

3.3. Conductivity–electric field strength relationships in capillary electrophoresis and capillary electrochromatography

Rathore et al also plotted the conductivity against the electric field strength, E, and E^3 as shown in Figs. 11 and 12 for the cases of open capillary and packed column, respectively [1]. As discussed earlier and seen in Figs. 11A and 12A, conductivity is not a constant, but increases with the electric field strength due to Joule heating for cases when the mobile phase contains 20% of 50 and 100 mM Tris. Further, it is seen in Figs. 11B and 12B that the data for these cases fits the proposed relationship in Eq. (22) very well and the conductivity increases in a linear fashion when plotted against E^3. The coefficient of linearity for all the plots was >99%. This is very consistent with the findings of Yu et al. [5] for open capillary capillary electrophoresis.

Table 6
Calculation of theoretical temperature inside a packed column at different voltages

Buffer	V (kV)	i (μA)	σ (mS cm^{-1})	ΔT_{ref} (K)	k	Bi'_{oA}	T (°C)
MeCN–100 mM Tris (80:20) (total Tris 20 mM)	5	2.79	0.474				25.0
	10	5.79	0.492	0.194	0.070		26.6
	15	9.16	0.519	0.437	0.105		28.9
	20	13.48	0.572	0.777	0.139		32.5
	25	19.21	0.652	1.215	0.174		38.1
	30	26.01	0.736	1.749	0.209	0.061	47.1
MeCN–50 mM Tris (80:20) (total Tris 10 mM)	5	1.17	0.199				25.0
	10	2.40	0.204	0.082	0.044		26.1
	15	3.73	0.211	0.183	0.066		27.4
	20	5.21	0.221	0.326	0.088		29.6
	25	6.93	0.235	0.509	0.111		32.6
	30	9.03	0.256	0.734	0.133	0.040	36.9
MeCN–10 mM Tris (80:20) (total Tris 2 mM)	5	0.26	0.044				25.0
	10	0.52	0.044	0.018	0.020		25.4
	15	0.79	0.045	0.040	0.030		26.0
	20	1.07	0.045	0.072	0.040		26.7
	25	1.37	0.047	0.112	0.050		27.8
	30	1.69	0.048	0.162	0.060	0.022	29.1

Column, 15 cm × 75 μm; packing, 1 μm bare silica; column porosity, 0.4; buffer pH, 8.0; thermal conductivity of solution of 0.61 W m^{-1} K^{-1} and temperature coefficient of electrical conductivity, α, as calculated in Table 4. Adapted from [1].
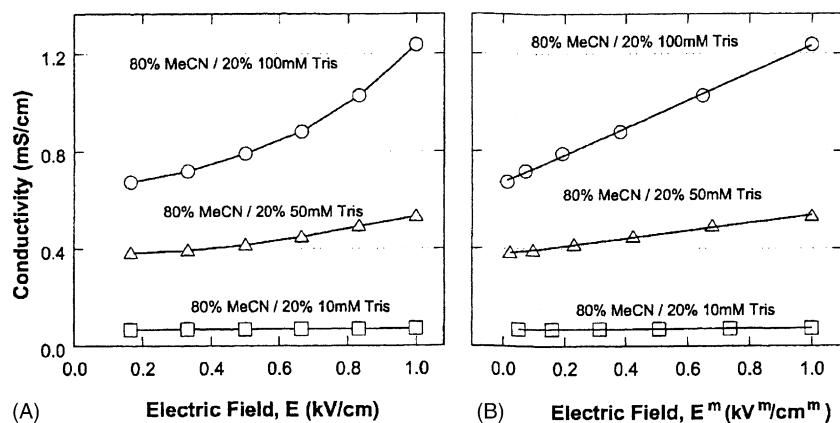
Fig. 11. Dependence of the electrical conductivity on: (A) electric field strength and (B) cube of the electric field strength as predicted by Eq. (22) for the case of an open capillary filled with different buffers (m is the fitted parameter of the equation and is equal to 3 in our calculations). Raw data are presented in Table 5. Silica capillary, 30 cm × 75 μm; buffer pH, 8.0 and detection at 214 nm.
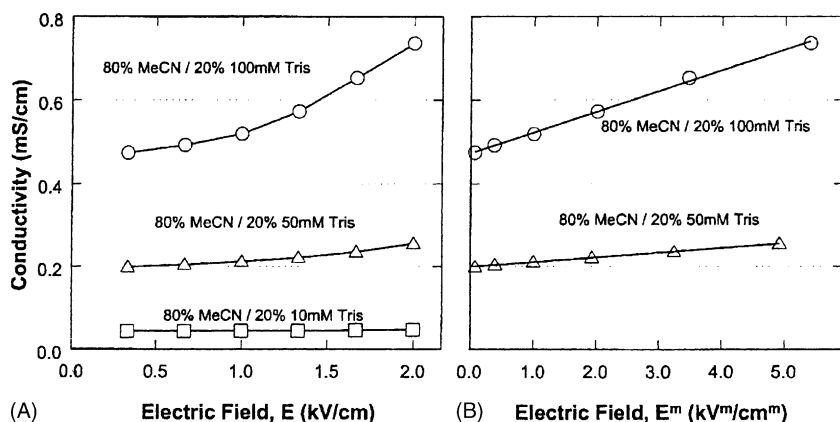

Fig. 12. Dependence of the electrical conductivity on: (A) electric field strength and (B) the electric field strength as predicted by Eq. (22) (m is the fitted parameter of the equation and is equal to 3 for our calculations) for the case of a 75 μm i.d. capillary column (15 cm) packed with 1 μm bare silica filled with different mobile phases. Raw data are presented in Table 6. Adapted from [1].

4. Concluding remarks

This article reviews the progress that has taken place in the past decade on the topic of estimation of Joule heating and temperature inside an open or packed capillary in electro-driven separation techniques of CE and CEC, respectively. Not many significant developments were found in the area of theoretical modeling of heat transfer in the capillary systems except for attempts to apply the existing models on newer techniques such as CEC and chip-based CE. However, the advent of novel analytical tools such as pulsed magnetic field gradient NMR, NMR thermometry, and Raman spectroscopy, have led to a revolution in experimental estimation of Joule heating and temperature inside the capillary via different non-invasive techniques. It is evident that while Joule heating will continue to plague electro-driven separations, clever choice of the buffer systems and design of the apparatus can significantly reduce the separation inefficiencies resulting from Joule heating. It can be concluded that the issue of Joule heating will continue to receive the due attention and consideration while the next generation separation tools, such as, laboratory-on-a-chip systems, are developed.

References

[1] A.S. Rathore, K. Reynolds, L.A. Colon, Electrophoresis 23 (2002) 2918.
[2] A.S. Cohen, A. Paulus, B.L. Karger, Chromatographia 24 (1987) 15.
[3] M.S. Bello, M. Chiari, M. Nesi, P.G. Righetti, M. Saracchi, J. Chromatogr. 625 (1992) 323.
[4] M.S. Bello, E.I. Levin, P.G. Righetti, J. Chromatogr. A 652 (1993) 329.
[5] L. Yu, J.M. Davis, Electrophoresis 16 (1995) 2104.
[6] E. Grushka, R.M. McCormick, J.J. Kirkland, Anal. Chem. 61 (1989) 241.
[7] H. Poppe, J.C. Kraak, J.F.K. Huber, J.H.M. van den Berg, Chromatographia 14 (1981) 515.
[8] J.H. Knox, K.A. McCormack, Chromatographia 38 (1994) 207.
[9] W.A. Gobie, C.F. Ivory, J. Chromatogr. 516 (1990) 191.
[10] M.S. Bello, P.G. Righetti, J. Chromatogr. 606 (1992) 95.

[11] M.S. Bello, P.G. Righetti, J. Chromatogr. 606 (1992) 103.

[12] R.F. Cross, J. Cao, J. Chromatogr. A 809 (1998) 159.

[13] S. Palonen, M. Jussila, S.P. Porras, T. Hyötyläinen, M.-L. Riekkola, J. Chromatogr. A 916 (2001) 89.

[14] K. Swinney, D.J. Bornhop, Electrophoresis 23 (2002) 613.

[15] S.P. Porras, E. Marziali, B. Gäs, E. Kenndler, Electrophoresis 24 (2003) 1553.

[16] U. Tallarek, E. Rapp, T. Scheenen, E. Bayer, H.V. As, Anal. Chem. 72 (2000) 2292.

[17] M.E. Lacey, A.G. Webb, J.V. Sweedler, Anal. Chem. 72 (2000) 4991.

[18] K.K. Llu, K.L. Davis, M.D. Morris, Anal. Chem. 70 (1998) 3744.

[19] R.J. Hunter, Foundations of Colloid Science, Clarendon Press, Oxford, 1986, p. 395.

[20] R.J. Hunter, Zeta Potential in Colloid Science Principles and Applications, Academic Press, London, 1988, p. 11.

[21] P.C. Hiemenz, R. Rajagopalan, Principles of Colloid and Surface Chemistry, Marcel Dekker, New York, third ed., 1997, p. 499.

[22] J.H. Masliyah, Electrokinetic Transport Phenomena, Aostra, Alberta, 1994, p. 99.

[23] A.S. Rathore, E. Wen, Cs. Horváth, Anal. Chem. 71 (1999) 2633.